Available online at www.sciencedirect.com

Catalysis Today 93–95 (2004) 223–228

www.elsevier.com/locate/cattod

The novel and highly selective fumed silica-supported VPO for partial oxidation of *n*-butane to maleic anhydride

C.Y. Xiao [a], X. Chen [a], Z.Y. Wang [a], W.J. Ji [a,*], Y. Chen [a], C.T. Au [b,*]

[a] *Mesoscopic Chemistry Lab, Department of Chemistry, Nanjing University, Nanjing 210093, PR China*
[b] *Department of Chemistry, Hong Kong Baptist University, HongKong, China*

Abstract

By applying fumed SiO_2 as support material, introducing the additive of polyethylene glycol (PEG) in the preparation medium and a deposition-precipitation method based on organic phase, we prepared the novel fumed SiO_2-supported VPO catalysts. The catalysts are the most selective in comparison to the various supported VPO counterparts for the partial oxidation of *n*-butane to maleic anhydride. At 653 K the derived samples showed butane conversion of 33–40% and MA selectivity of 87–65 mol%. The catalysts not only showed good performance at lower reaction temperatures, but also maintained higher MA selectivity at different loadings. In addition to the unique nature of fumed SiO_2, the highly uniform dispersion of VPO component and the involved VPO-support interaction, co-existence of predominant $(VO)_2P_2O_7$ phase and minor $VOPO_4$ may also be beneficial to the good performance on the unique fumed SiO_2-based catalysts. In addition, broadening of the (2 0 0) diffraction line of $(VO)_2P_2O_7$ phase is an indication of structural disorder, one considered to be relevant to MA formation.

Keywords: Fumed SiO_2; Supported VPO; Partial oxidation; *n*-Butane; Maleic anhydride

1. Introduction

Selective oxidation of *n*-butane to maleic anhydride (MA) is currently the only commercialized process for light paraffin conversion, and the effective catalysts are primarily unsupported vanadyl pyrophosphate, $(VO)_2P_2O_7$ [1,2]. Supported catalysts, however, have several potential advantages over the unsupported ones, and attempts to prepare supported VPO catalysts on SiO_2, TiO_2, and Al_2O_3 have been reported [3–6]. The use of support, however, may introduce support–oxide interactions that could hinder the formation of the active $(VO)_2P_2O_7$ phase, and the resulted catalysts generally exhibited low butane conversion and poor MA selectivity [7–9]. The type and/or nature of support materials showed a significant influence on reaction performance. When there is a strong interaction between VPO and a reducible support, such as titania and zirconia, the VPO components became more reducible, and enhancement in catalytic activity is remarkable. On the other hand, the application of a support such as silica that interacts less strongly with the active phase/species, would improve the selectivity but decrease the conversion. Harding et al. reported that an MA selectivity of 50% can be achieved by adopting an unusually high P/V ratio of greater than 2 in the catalysts [10]. Previously, we prepared supported VPO catalysts on MCM-41 and SiO_2 of large pore, and found that the MCM-41-supported VPO specimen at an appropriate VPO loading showed considerably improved MA selectivity [11]. It was also found that the medium (aqueous or organic) for catalyst preparation had a great effect on the behavior of the catalyst [12]. In this study, we adopted fumed SiO_2, a unique kind of silica which is non-porous in the primary particles, with optimized synthesis method to prepare a new kind of supported VPO for the target reaction. The results of characterization and evaluation of this series of catalysts are reported.

2. Experimental

2.1. Catalyst preparation

The deposition-precipitation method for catalyst preparation in an organic medium is according to a recent Chinese

---

* Corresponding authors.
E-mail addresses: jiwj@nju.edu.cn (W.J. Ji), pctau@hkbu.edu.hk (C.T. Au).

0920-5861/$ – see front matter © 2004 Elsevier B.V. All rights reserved.
doi:10.1016/j.cattod.2004.06.127

patent [13]. Briefly speaking, the catalyst precursor was prepared in an organic medium by the reaction of V_2O_5 with a mixture of *iso*-butanol and benzyl alcohol (volume ratio of 1:1). After the reaction mixture was refluxed at 413 K for 5 h, certain amount of PEG 20,000 was added and then the fumed SiO_2 material was introduced. The reaction mixture was refluxed for 1 h, and phosphoric acid was added at a vanadium/phosphorus ratio of 1.0/1.2. After refluxing for another 6 h, the turbid reaction mixture was filtered. The resulted precipitate was washed with *iso*-butanol and acetone, respectively; then dried in air at 393 K for 24 h. The dried precursor was in situ activated in the reaction mixture of 1.5% *n*-butane/air at a rate of 2 K/min from room temperature to 673 K and kept at this temperature for 15 h to obtain the fresh activated catalyst.

2.2. Characterization

The characterization of the freshly activated samples was conducted by means of BET, XRD, XPS, SEM, and TPR measurements. Specific surface areas were measured by nitrogen adsorption–desorption at 77 K on the Micromeritics ASA2000 apparatus. X-ray diffraction patterns were recorded at room temperature using a Shimadzu XD-3A diffraction meter with Graphite-filtered Cu Kα radiation. The samples were mounted on a mylar foil using Vaseline, and X-ray tube was operated at 35–40 kV and 100–200 mA. XPS measurement was performed on an X-ray photoelectron spectrometer VG ESCALAB MK II, with 1253.6 eV (Mg Kα) radiation at a setting of 12 kV and 20 mA. The binding energies (BE) were calibrated against the C 1s signal (284.6 eV) of contaminant carbon. Removal of O 1s satellite and curve-fitting of the V $2p_{3/2}$ peak were performed by using the SCAKAB software. The surface concentrations of the elements were estimated on the basis of the corresponding peak areas normalized by using the Wagner Factor database. The morphology of the samples was examined on an SEM-200 Scanning Electron Microscopy (JEOL). Temperature-programmed reduction (TPR) was performed within the temperature range of 298–1023 K, and ∼150 mg sample was placed in a quartz reactor and reduced in a mixture of 7.2% H_2 in balanced N_2 at a rate of 10 K/min. Raman spectra were collected on a LABRAM-HR Raman spectrometer at room temperature with excitation source of 513 nm and power of 1.5 mW.

2.3. Catalyst evaluation

Catalytic performance for partial oxidation of *n*-butane to MA was evaluated in a quartz fixed-bed micro-reactor (Φ = 8 mm) with a continuous down-flow. The samples were pressed to pellets and then crushed and sieved. Typically, 0.5 g 25–40 mesh sample was used for the reaction. The feed composition was 1.5% $n\text{-}C_4H_{10}$, 17.5% O_2 and balanced N_2. The gas hourly space velocity (GHSV) was ca. 1200 h^{-1}. On-line gas chromatography system was used to analyze the outlet mixture; the carbon balance was usually better than 95%.

3. Results and discussion

The surface area of the fumed SiO_2 support is 250 m^2/g, and the surface areas of the 15, 28, and 57% VPO/fumed SiO_2 samples are 206, 178, and 117 m^2/g, respectively. Apart from the effect of increasing content of VPO and decreasing content of the support in the sample, the presence of VPO phase does not notably affect the surface area of fumed SiO_2. The surface of samples will increase with increasing VPO content if the amount of silica is taken constant in the samples, and this is due to the contribution of the VPO phase to the surface area. On the other hand, even at 57% VPO content, the sample showed the surface area of 117 m^2/g, indicating that the porosity between the primary particles of fumed SiO_2 was roomy for the accommodation of supported VPO. The results of XRD studies are shown in Fig. 1. It was found that even at low loadings, the supported VPO component existed mostly in the form of $(VO)_2P_2O_7$ phase, differing considerably from that observed over other supported VPO catalysts [3–6,11–14]. Birkeland et al. [3] and Bueno et al. [6] reported that the α-$VOPO_4$, γ-$VOPO_4$, and $VO(SiO)P_2O_7$ phases could form in large quantities in the conventional SiO_2-supported VPO samples, especially when the samples were prepared in aqueous media. On the Al-containing MCM-41-supported samples, the VPO component was found to be in amorphous form even at high loadings [11], while on a SiO_2-supported sample of large pores, some $(VO)_2P_2O_7 \cdot H_2O$ phase would appear at high loadings [12]. When the VPO component was deposited on the silica support by means of electrochemical process, Overbeek et al. reported that the supported VPO was also in amor-

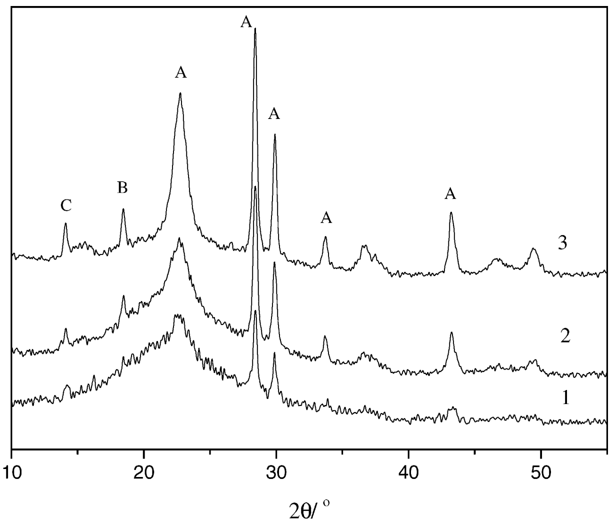

Fig. 1. XRD patterns of (1) 15% VPO/fumed SiO_2; (2) 28% VPO/fumed SiO_2 and (3) 57% VPO/fumed SiO_2. (A) $(VO)_2P_2O_7$; (B) γ-$VOPO_4$; (C) $VO(H_2PO_4)_2$.

phous state [13,14]. These results reflect the difference in texture and other characteristics between fumed SiO_2 and conventional SiO_2, large-pore SiO_2 as well as MCM-41. Besides the major $(VO)_2P_2O_7$ phase, there appears other minor phases, namely $VO(H_2PO_4)_2$ and γ-$VOPO_4$ in the fumed SiO_2-supported samples, and these minor phases may have an impact on the overall reaction performance even in small quantities.

The XPS technique was adopted for the investigation of surface properties, and the results are summarized in Table 1. The V $2p_{3/2}$ binding energies for V^{4+} in $(VO)_2P_2O_7$ and V^{5+} in $VOPO_4$ are found to be 516.6 and 517.7 eV, respectively [14]. From Table 1 it was found that the binding energies of the elements of V, P, and O for the VPO/fumed SiO_2 catalysts are close to the values reported for $(VO)_2P_2O_7$ [14], suggesting that the oxidation state of the major vanadium phase is 4+. It was also revealed that the element of P was enriched on the surface, and this is a common phenomenon observed on unsupported VPO catalysts [15,16]. Note that the BE of vanadium increased at high VPO loading, indicating more amount of V^{5+} phase existing in the high loading sample, and this is in concord with the XRD observation. Note also that the surface V/Si ratio obtained in XPS measurement was fairly low, implying that a large portion of VPO could be enclosed inside the fumed SiO_2 support and was hardly detected by XPS. In Table 1, the data for another VPO/TiO_2–SiO_2 supported sample (28% loading) are also included for comparison. It can be seen that both the binding energies of the elements of V, P, and O as well as the ratios of P/V and V/Si are notably different from those of the fumed SiO_2-supported samples. In other words, the characters of the supported component are greatly determined by the nature of support material as well as the strength of interaction between oxide and support.

The Raman spectra of the samples are presented in Fig. 2. It is found that the Raman signals are rather weak for all the samples, which may be due to the nature of the fumed SiO_2 support. The Raman signals increased with increasing VPO loading. The major band at ca. 920 cm^{-1} could be due to the $\nu_{as,P\text{–}O\text{–}P}$ in $P_2O_7^{2-}$ unit of $(VO)_2P_2O_7$, and the rather weak bands at 1130 and 1180 cm^{-1} are the characteristics of the $(VO)_2P_2O_7$ species [17,18]; it is also likely to be the evidence for the presence of the $(VO)_2P_2O_7$ component inside the samples. Unfortunately, due to weak Raman signals, it is impossible to obtain information related to V^{5+} species.

Table 1
Binding energies, surface P/V and V/Si atomic ratios of the fumed SiO_2-supported samples

Sample	BE (eV)			P/V	V/Si
	V $2p_{3/2}$	P 2p	O 1s		
15% loading	516.6	133.6	532.4	1.5	0.02
28% loading	517.1	134.2	532.7	1.3	0.04
28% loading[a]	516.8	133.7	532.4	1.5	0.16
57% loading	517.1	134.2	532.6	1.8	0.10

[a] On the TiO_2–SiO_2 support (atomic ratio of Ti/Si = 0.04), data listed for comparison.

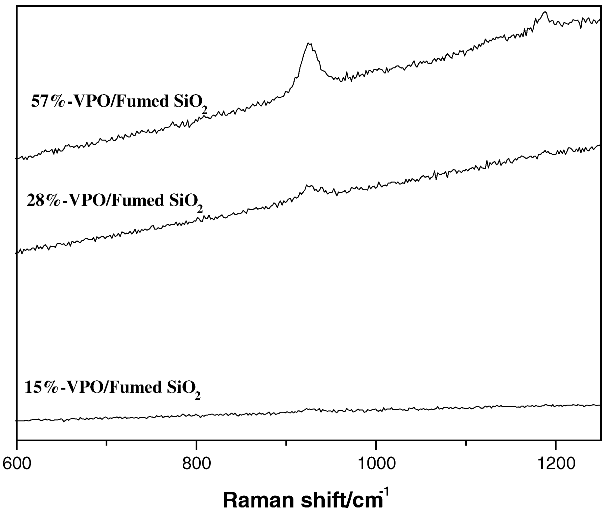

Fig. 2. Raman spectra of the fumed SiO_2-supported VPO catalysts.

The SEM photographs showed the morphology of the fumed SiO_2-supported samples (Fig. 3). The small plate-like species adhered to the aggregated particles of fumed SiO_2 are recognized the $(VO)_2P_2O_7$ phase and they are one of the typical morphologies observed. The number of plate-like particles of $(VO)_2P_2O_7$ is limited in the loading sample, and increased notably with increasing VPO content. Interestingly, even in the sample of highest VPO loading, the particle size of VPO component does not enlarge remarkably, while the quantity of VPO particles is considerably increased (Fig. 3(c)); indicating that the distribution of VPO component is highly uniform in these PEG-derived fumed SiO_2-supported samples due to the function of the applied PEG additive [19].

The partial oxidation of *n*-butane on VPO catalyst is known to proceed via a redox mechanism [2]; therefore, the reduction property of a catalyst is a key factor accounting for reaction behavior. The reduction behavior of a catalyst can be examined by means of the temperature-programmed reduction (TPR) technique. For the partial oxidation of *n*-butane, the redox cycle of vanadium only involves the reduction of V^{4+} and V^{5+}, and the further reduction of V^{3+} is not the main concern of this study. Therefore, the adopted temperature range (from RT to 1023 K) for TPR is usually sufficient for reduction of V^{4+} and V^{5+} according to our previous studies [11,19]. One can see from Fig. 4 that the consumption of H_2 starts at around 673 K but the major reduction process of V^{4+} in $(VO)_2P_2O_7$ phase is not completed as the temperature is raised to 1023 K. After being held in the reducing atmosphere at 1023 K for ~45 min, the reduction of V^{4+} is nearly completed. It is apparent that reduction of V components (V^{4+} as well as V^{5+}) supported on fumed SiO_2 is more difficult as compared to the unsupported VPO counterparts [19] or to the ones supported on Al-containing MCM-41 [11]. In addition, the reducibility (on the basis of

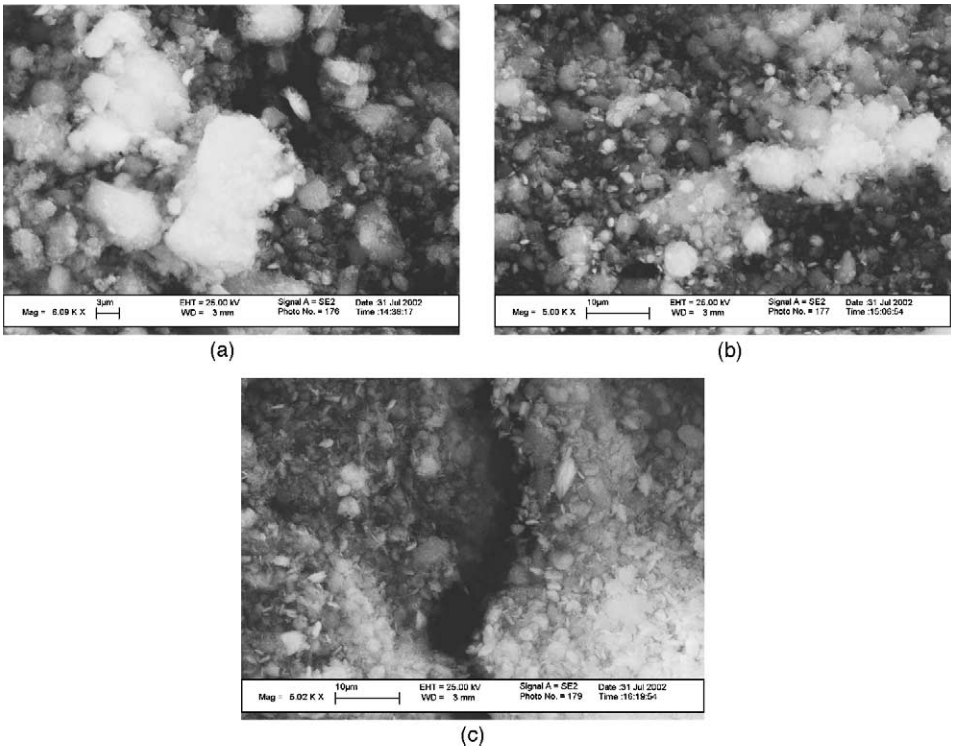

Fig. 3. SEM of (a) 15%-, (b) 28%- and (c) 57% VPO/fumed SiO_2 catalysts.

the content of reduced VPO) decreased, and the onset temperature for reduction shifted to higher temperatures with increased loadings, indicating that there is an obvious variation in the strength of oxide–support interaction with loading, which in turn shows an effect on the reduction behavior of the supported component. The V^{5+} cations of $VOPO_4$ specimen are reduced at lower temperatures, as evidenced by the asymmetrical shape of the major reduction peak over the samples of higher loadings. It is clear that the interaction between the VPO component and fumed SiO_2 support varies with both the nature of support and VPO loading, and hence affects the reduction property of lattice oxygen.

The fumed SiO_2-supported VPO catalysts show exceptional performance for the target reaction (Table 2 and Fig. 5), and the typical catalytic performance at 653 K are 33–40% of *n*-butane conversion and 87–65 mol% of MA selectivity, giving 26–29 mol% MA yield. Generally speaking, butane conversion increased with increasing reaction temperature, but such increment was not significant. On the other hand, MA selectivity increased with increasing VPO loading but declined gradually at elevated temperatures. Under the same reaction conditions, unsupported VPO catalyst showed ca. 35 mol% of MA yield, with 56% of butane conversion and 63 mol% of MA selectivity, respectively. On the basis of per unit mass of catalyst, the performance of

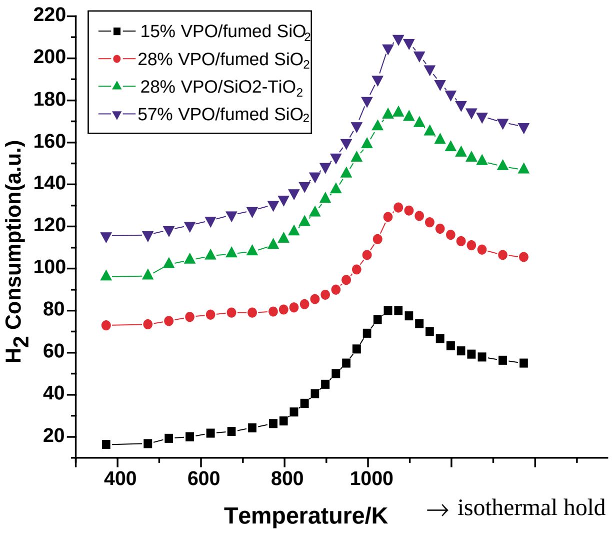

Fig. 4. TPR profiles of the supported VPO catalysts on fumed SiO_2 as well as SiO_2–TiO_2.

Table 2

The reaction performances of the fumed SiO_2-supported VPO catalysts

Sample	Temperature (K)	Conversion (%)	Selectivity (mol%)	Yield (%)
15% loading	613	19.2	90.5	17.4
	633	28.1	77.9	21.9
	653	39.4	64.5	25.4
28% loading	613	20.3	95.0	19.3
	633	27.2	83.2	22.6
	653	38.3	71.3	27.3
57% loading	613	16.7	96.2	16.1
	633	23.9	93.3	22.3
	653	33.0	87.5	28.8

Table 3
Comparison of the specific activity and MA selectivity for the VPO/fumed SiO_2 samples and unsupported catalyst at 653 K

Sample	15% loading	28% loading	57% loading	Unsupported
Specific activity[a] ($\mu mol\,g^{-1}\,(VPO)\,min^{-1}$)	41.6	24.0	12.4	8.6
MA Selectivity (mol%)	64.5	71.3	87.5	63

[a] The activity is normalized to per unit mass of VPO loading.

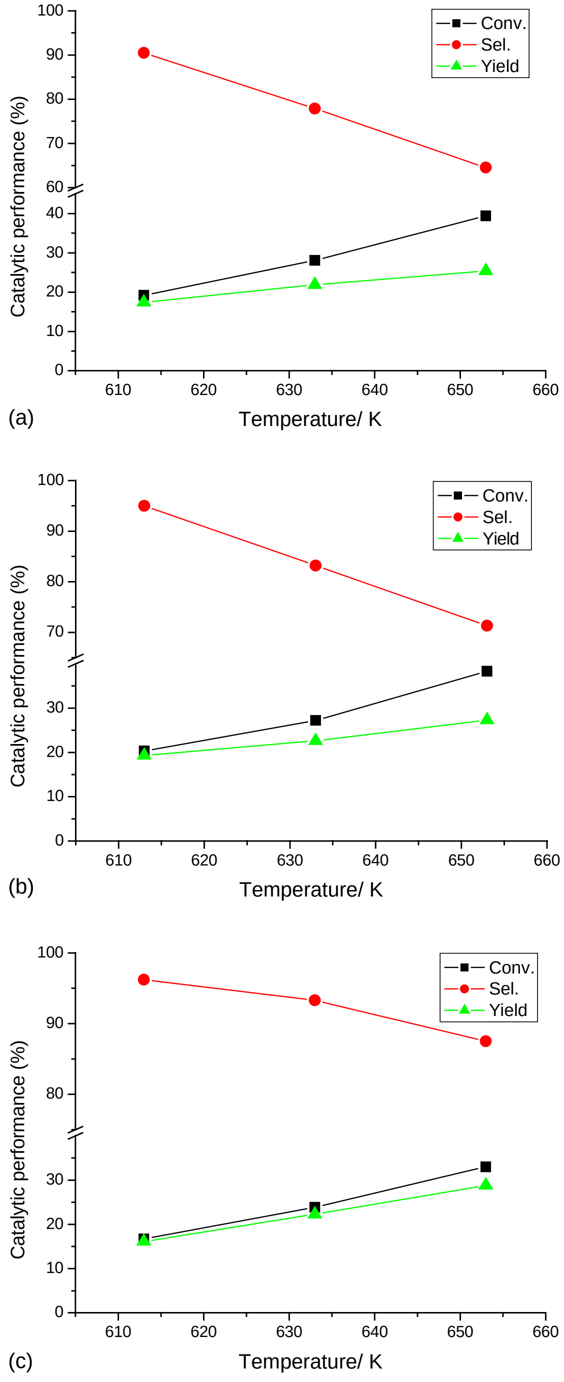

Fig. 5. The reaction performances of (a) 15%-, (b) 28%- and (c) 57% VPO/fumed SiO_2 catalysts.

the fumed SiO_2-based catalysts is only slightly inferior to that of the unsupported one. However, this performance is better than that of our VPO/MCM-41 and VPO/large-pore SiO_2 catalysts [11,12] and also superior to those reported on the conventional SiO_2 and other supported VPOs under similar conditions [4,5,20]. In order to compare the performance more strictly, the data of specific activity (normalized to per unit mass of VPO loading) were also presented in Table 3. The deviation in specific activity and MA selectivity again suggested that the nature of VPO component not only change with the VPO content in the fumed SiO_2-based samples but also be different from that of unsupported VPO catalyst. Note that the catalysts showed comparatively good performance even at notably lower reaction temperatures, while high MA selectivity could be maintained over the serial samples of different loadings. Significantly lower reaction temperature actually also ensures high MA selectivity and low energy consumption. At the indicated level of butane conversion, the fumed SiO_2-based catalysts are the most selective among the various supported VPO counterparts. As revealed by XRD and SEM, the highly uniform dispersion of VPO component with which the dominant $(VO)_2P_2O_7$ phase plus minor $VOPO_4$ can be obtained in the fumed SiO_2-based samples, and this may be the result of the function of additive of PEG, the unique nature of fumed SiO_2 and the interaction between VPO component and the adopted support. Co-existence of dominant $(VO)_2P_2O_7$ and minor $VOPO_4$ in these fumed SiO_2-based catalysts may be beneficial for MA formation, while the dispersion of $VOPO_4$ may also be influential for the performance. This preposition was supported by our previous observations made on serial PEG-derived unsupported VPO samples [21]. In addition, according to XRD results, the (2 0 0) diffraction peak of $(VO)_2P_2O_7$ phase is notably broadened, which could be owing to both the possible structural disorder of VPO component and the contribution of the silica support. This structural disorder could be induced by alcohol intercalation into the VPO precursor since additional alcohol was used for catalyst preparation, which may be relevant to MA formation [22–24].

Acknowledgements

We acknowledge the financial supports from the Ministry of Science and Technology of China (G2000048009), the High-Tech Project of Jiangsu Province (BG2001038), and the Hong Kong Baptist University (FRG/02-03/I-17).

References

[1] B.K. Hodnett, Catal. Rev.-Sci. Eng. 27 (1985) 373.
[2] G. Centi, F. Trifiro, J.R. Ebner, V.M. Franchetti, Chem. Rev. 88 (1988) 251.
[3] K.E. Birkeland, S.M. Babitz, G.K. Bethke, H.H. Kung, G.W. Coulston, S.R. Bare, J. Phys. Chem. B 101 (1997) 6895.
[4] R.A. Overbeek, A.R.C.J. Pekelharing, A.J. van Dillen, et al., Appl. Catal. A 135 (1996) 231.
[5] R.A. Overbeek, P.A. Warringa, M.J.D. Combag, et al., Appl. Catal. A 135 (1996) 209.
[6] J.M.C. Bueno, G.K. Bethke, M.C. Kung, H.H. Kung, Catal. Today 43 (1998) 101.
[7] V.A. Zazhigalov, Y.P. Zaitsev, V.M. Belousor, B. Parlitz, W. Hanke, G. Ohlman, React. Kinet. Catal. Lett. 32 (1986) 209.
[8] N.T. Do, M. Baerns, Appl. Catal. 45 (1988) 1.
[9] N.T. Do, M. Baerns, Appl. Catal. 45 (1988) 9.
[10] W.D. Harding, K.E. Birkeland, H.H. Kung, Catal. Lett. 28 (1994) 1.
[11] W. Nie, X. Wang, W. Ji, Q. Yan, Y. Chen, C.T. Au, Catal. Lett. 76 (2001) 201.
[12] W. Nie, Z. Wang, W. Ji, Q. Yan, Y. Chen, C.T. Au, Appl. Catal. A: Gen. 244 (2003) 265.
[13] W. Ji, X. Chen, Z. Wang, Y. Chen, Chinese Patent 03131515.1 (2003).
[14] M. Abon, K.E. Bere, A. Tuel, P. Delichere, J. Catal. 156 (1995) 28.
[15] G. Centi, F. Trifiro, J.R. Ebner, V.M. Franchetti, Chem. Rev. 88 (1988) 55.
[16] L.M. Cornaglia, C. Caspani, E.A. Lombardo, Appl. Catal. 74 (1991) 15.
[17] A.F. Ben, R. Oliver, N. Guillaume, F. Lefebvre, J.C. Volta, J. Catal. 134 (1992) 151.
[18] V.V. Guliants, J.B. Benziger, S. Sundaresan, I.E. Wachs, J.M. Jehng, J.E. Roberts, Catal. Today 28 (1996) 275.
[19] X. Wang, L. Xu, X. Chen, W. Ji, Q. Yan, Y. Chen, J. Mol. Catal. A: Chem. 206 (2003) 201.
[20] M. Ruitenbeck, A.J. van Dillen, A. Barbon, E.E. van Faassen, D.C. Koningsberger, J.W. Geus, Catal. Lett. 55 (1998) 133.
[21] X. Wang, X. Chen, W. Ji, B. Li, Q. Yan, Y. Chen, J. Phys. Chem. B, revised.
[22] G. Busca, F. Cavani, G. Centi, F. Trifio, J. Catal. 99 (1986) 400.
[23] P.G. Pries de Oliverira, J.G. Ebon, M. Chavant, A.S. Riche, V. Martin, S. Caldaelli, J.C. Volta, Catal. Today. 57 (2000) 177.
[24] G. Busca, G. Centi, J. Amr. Chem. Soc. 111 (1989) 46.